Brake Efficiency on Private Passenger Vehicles Using Finite Element Method: A Research in Traffic Efficiency

Haodong Hu

March 26, 2021

Abstract

In engineering studies, Linear Vibration represents the phenomenon where all basic components of a vibratory system, such as spring and contacting surfaces, behave linearly. In other words, its resulting sound will always be sustained and range within specific range. This paper will interpret the concept of linear vibration mathematically through polar and cylindrical coordinates. Then, we will integrate Finite Element Method (FEM) and corresponding partial differential equations (PDE) into the two coordinate systems in order to analyze brake efficiency on private passenger vehicles based on the idea of linear vibration. Furthermore, the paper will provide detailed examples and explanations of how FEM and PDEs are used mathematically and how they have contributed to the process of brake analysis. One of the cores of this research also contributes to traffic efficiency. Traffic efficiency particularly at intersections, is a critical factor in urban transportation systems, impacting travel times, fuel consumption, and overall roadway safety. While numerous factors contribute to traffic flow dynamics, the mechanical performance of individual vehicles plays a significant role. Among these, the brake efficiency of private passenger vehicles is a crucial yet often overlooked element influencing traffic efficiency at intersections and across networks of multiple intersections. Brake efficiency refers to a vehicle's ability to decelerate effectively and predictably in response to driver input, which depends on factors such as brake system condition, tire-road interaction, and environmental conditions. Inconsistent or suboptimal braking performance in private passenger vehicles can lead to erratic behavior at intersections, where precision and coordination among vehicles are paramount. Vehicles with poor brake efficiency may require longer stopping distances, fail to adhere to signal timing, or create unexpected delays, disrupting the smooth flow of traffic. At signalized intersections, traffic flow heavily depends on the synchronization of vehicle movements and adherence to green-light intervals. A vehicle that fails to stop promptly may block cross-traffic, causing bottlenecks or collisions. Similarly, during peak hours or at intersections with complex phasing, vehicles with inconsistent braking performance can lead to hesitations and over-cautious driving by others, further reducing throughput. These disruptions are magnified in multi-intersection networks, where delays propagate downstream, causing cascading congestion. Moreover, the effects of brake efficiency extend beyond individual intersections. In arterial traffic flow systems, where multiple intersections are closely spaced and often coordinated through adaptive signal control systems, poor braking performance can distort the timing offsets. This misalignment results in reduced green-wave effectiveness, increased idling times, and overall inefficiencies in traffic management. Understanding the interplay between vehicle brake efficiency and traffic dynamics is essential for improving urban traffic systems. By addressing how braking performance affects stop-and-go cycles, queue formation, and intersection capacity, planners can identify strategies to enhance efficiency. This research aims to investigate these relationships, providing insights into the systemic impact of brake efficiency on traffic at intersections and offering potential mitigation strategies, including vehicle maintenance campaigns, traffic signal optimization, and the integration of advanced driver-assistance systems (ADAS).

1 Introduction

Finite Element Method (FEM) is a widely used method for numerically solving differential equations arising in mathematical modeling. To solve a problem, the FEM subdivides a large system into smaller, simpler parts that are called finite elements. In mathematics, it is important to visualize and analyze a single element (problem) within a specific "context", and therefore, we use PDEs to first reduce the dimension of certain

system (subdividing into simpler parts) and then fit each part into a polar or cylindrical coordinate system before utilizing specific strategy for each part of the subject to determine their design flaws and weaknesses.

It is reported that the generation of brake squeal (500-1000Hz) has caused tremendous customer dissatisfaction in automobile industry, which, as a result, could jeopardize the reputation of certain automobile companies and therefore, damage the sale of their products[7]. Moreover, experiments[2][12][9] have suggested that persistent brake squeal will tremendously reduce the performance of the brake system and therefore, threaten the safety of the operator.

The earliest studies on brake squeal using FEM and PDEs can be dated back to 1930s, where Johann Hadji Argyris integrated the solutions of PDEs into a matrix and discovered the relationship between surface of disc and its corresponding sound frequency based on the eigenvalues of the matrix[5]. Moreover, K.Feng, a Chinese mathematician, developed a systematic numerical method of solving differential equations especially for brake squeal[5]. Apparently, these studies have been very crucial in terms of understanding and optimizing the phenomenon of brake squeal, and this paper will continue to analyze the issue based on previous results but from a different perspective (linear vibration analysis) and state several main results obtained by such method.

In section 2, we will introduce the concepts of PDEs and why it is useful in terms of brake squeal analysis. Then, there will be a brief example of how the combination of strong and weak forms of PDEs are used to reduce the dimension of a problem and therefore, obtain the most accurate result without compromising the efficiency. Section 3 will provide several basic concepts and terms of a typical rotor brake system. Also, it will explain how the brake system works during a braking operation. Section 4 focuses on modeling the brake rotor by transferring the equation of motion mathematically using the Young's Modulus (4.1) and Poisson's Ratio (4.3). Then, we will use Lagrangian Coordinate (4) and Kronecker Product (4.5) to simplify the equation and derive a new formula that could potentially indicate the relationship between brake rotor and vibration frequency. In section 5, we will rigorously analyze the two equations that are derived in section 4 based on linear vibration analysis. Then, it will conclude the paper by reiterating all of the observations and results from previous sections (together with the calculations of determinants and eigenvalues of different matrices) in order to determine the main cause of brake squeal.

2 Finite Element Method and PDEs

In this section, we will begin by defining several key terms that will be utilized throughout the paper, and then, we will show an example of how PDEs are used in FEM in terms of dimension reduction.

Definition 2.1. *The Strong Form* of a PDE evaluates the partial derivatives without specifying the boundary conditions requirements and the solution is not exact. For example, the general form for second partial derivative is

$$f_{xy} = \frac{\partial^2 f}{\partial x \partial y}$$

where this means to take the partial derivative first with respect to y and then with respect to x in the function f.

Since it could be complicated to find the exact solution of a PDE in its strong form, we need to first approximate the solution within specific interval and then, based on the solution obtained, we begin to expand the interval until we have a sustained solution, and this is where we need to use the *weak form*[5] of the PDEs.

Definition 2.2. *The Weak Form* of a PDE reduces the continuity requirements on the basis functions used for approximation which gives way to using lesser degree polynomials, which is done by converting the differential equation into an integral form which is usually easier to solve comparatively. In general, given the boundary for $x \in [a, b], y \in [c, d]$, the strong form of the PDE can be interpreted in the form

$$v(x) = \int_c^d \int_a^b f_{xy} dx dy$$

Remark 2.3. The weak form of PDEs does not imply "inaccuracy" or "inferiority".

The following is an example of the transformation from the strong form of the PDE to its weak form[6].

Example 2.4. Here is a strong form of a PDE

$$\frac{d}{dx}\left(-a\frac{du}{dx}\right) = f$$

where $u(0) = 0$, $-au_x(1) = -Q$ and u_x means to take the derivative of x in the function of u. To convert it into weak form, we first multiply ODE by a function $u^v(x)$ that satisfies $u^v(0) = 0$:

$$(-au_x)_x u^v = fu^v$$

and in order to further simplify the above equation, recall the shift derivative[14] of $(-au_x)_x u^v$ can be represented as

$$(-au_x u^v)_x \equiv (-au_x)_x u^v + (-au_z)u_x^v$$

therefore, by plugging in $(-au_x)_x u^v + (-au_z)u_x^v$ to the left hand side of $(-au_x)_x u^v = fu^v$, we have

$$(-au_x u^v)_x - (-au_x)u_x^v = fu^v$$

then according to the definition of the weak form of PDE (2.2), we need to identify a specific interval for the strong form and then do the integration, and the general strategy is to set the boundary condition to be $[0, 1]$, and we have

$$\int_0^1 (-au_x u^v)_x dx - \int_0^1 (-au_x)u_x^v dx = \int_0^1 fu^v(x)dx$$
$$[-au_x u^v]\Big|_0^1 + \int_0^1 au_x u_x u^v dx = \int_0^1 fu^v(x)dx$$

then we plug in the given boundary conditions for $(-au_x u^v)_x$ so we get a new expression

$$-Qu^v(1) + \int_0^1 au_x u_x^v dx = \int_0^1 fu^v(x)dx$$
$$\int_0^1 au_x u_x^v dx = \int_0^1 fu^v(x)dx + Qu^v(1)$$

in this case, we have successfully transformed the strong form of PDE to its weak form, and in order to approximate the solution of $\int_0^1 au_x u_x^v dx$, we only need to find the exact solution of $\int_0^1 fu^v(x)dx$ for $\forall u^v(x)$ where $u^v(0) = 0$ such that

$$\int_0^1 au_x u_x^v dx = \int_0^1 fu^v(x)dx + Qu^v(1)$$

In the later linear vibration analysis using FEM, we will utilize similar strategy in order to reduce the dimension of a given problem (PDE) and therefore obtain the most accurate result without compromising the efficiency of the process.

3 Background on Rotor Brake Components

In this section, we will introduce several basic components of a rotor brake system as well as each of their functions. Also, we will list several key steps for FEM and linear vibration analysis.

According to the market research report, the phenomenon of brake squeal often occurs in a rotor (disc) brake system[4], which is also the most common braking system utilized in the automobile industry. For a typical rotor brake system[6], the rotor is securely mounted on the axle hub so that it would rotate with the wheel of an automobile. The brake pads that composed of frictional material are compressed against

backing plates in order to generate a frictional torque to slow the rotation of rotor and wheel. In the end of this section is a simplified rotor brake system.

Therefore, the aim of this paper is to subdivide an automobile brake system according to their mechanical components, namely brake pads, brake rotors, backing plates, and pistons, and implement FEM to first model the brake rotor, which serves as the foundation for linear vibration analysis, and then, based on the existing results, the paper will focus on discussing the effects of temperature, friction, and wear during the operation.

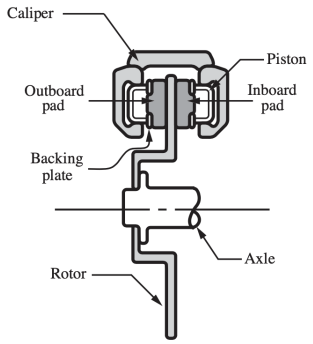

Figure 1: Cross-section of a simplified rotor brake system. The caliper houses the hydraulic pistons that actuate the brake pads, and wheel (not shown) is attached to the rotor

4 Modeling Brake Disc

Brake squeal is generated by the vibration of an unstable vibration mode of the brake system. In this condition the brake rotor can act as a loudspeaker since it has large flat surfaces that can readily radiate sound[13]. However, Modeling a disc brake assembly with the aim of eventually understanding its vibrations and dynamics is complicated by the fact that the brake disc is rotating and the pads and caliper are fixed. Therefore, in order to understand the issues associated with the vibration of the brake rotor, it is important to start with the discussion of a motionless plate model.

But before we actually get into the modeling procedures, please recall the basic definition of a *Polar Coordinate System*[6], which is a two-dimensional coordinate system in which each point on a plane is determined by a distance from a reference point and an angle from a reference direction. For instance in the Cartesian coordinate system at point is given the coordinates (x, y) and we use this to define the point by starting at the origin and then moving x units horizontally followed by y units vertically. Also notice that r is a straight line that connects the point and the origin, while θ measures the angle between x axis and the line r. This can be visualized in the sketch below.

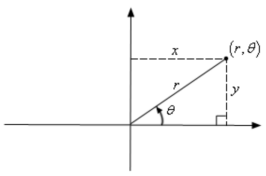

Figure 2: The variables x and y are in the horizontal and vertical axis respectively, and for any point on the coordinate system, it can be either represented by (x, y) or (r, θ)

Therefore, we could define the *Cylindrical Coordinate* system [6] as an extension of polar coordinate(4) into three dimensions. Moreover, not only is it an extension of polar coordinates, but we extend it into the

third dimension just as we extend Cartesian coordinates into the third dimension. All that we do is add a z, and θ and r remain the same as they are in polar coordinate. Below is a sketch of a point in $\mathbb{R}^3$.

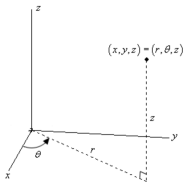

Figure 3: Similar in Figure 4, we can describe a point using r, θ, z, where r is the length between the origin and a point, θ is the angle between r and x axis, and z represents the z axis of cylindrical coordinate

In this paper, the rotor is modelled as a uniform circular plate of thickness h, inner radius r_i, and outer radius r_0[6].The inner radius is assumed to be fixed (or clamped) to a rigid axle. For any point of the disc, the displacement vector $\mathbf{u}$ can be expressed as

$$\mathbf{u} = u_R(R,\theta,z,t)\mathbf{e}_r + u_\theta(R,\theta,z,t)\mathbf{e}_\theta + u_z(R,\theta,z,t)\mathbf{e}_z$$

where R is the length between a point and the origin, θ is the angle between R and x axis, and z is the z axis of the cylindrical polar coordinate system(4). Also notice that the unit vectors are $\mathbf{e}_r = \cos(\theta)\mathbf{E}_x + \sin(\theta)\mathbf{E}_x$ and $\mathbf{e}_\theta = -\sin(\theta)\mathbf{E}_x + \cos(\theta)\mathbf{E}_y$, and $\mathbf{E}_x, \mathbf{E}_y, \mathbf{E}_z$ are the eigenvectors with respect to x, y, z basis respectively. We also assume that $\mathbf{e}_z$ points along the rigid axle and the displacements u_R and u_θ are known as the in-plane or longitudinal displacements of the disc.

Following is the definition of Young's Modulus[3], and it is important to notice that The Young's Modulus (4.1) is in essence the stiffness of a material. In other words, it calculates how easily one object can be bended or stretched.

Definition 4.1. In practice, if we denote Young's Modulus as E, then $E = \frac{\text{stress}}{\text{strain}} = \frac{\sigma}{\mathcal{E}}$, where stress (denoted as σ) is the force exerted on the object and strain (denoted as $\mathcal{E}$) is change in length with respect to the original length.

Remark 4.2. In Mathematics, the Young's Modulus can be calculated by polar coordinate.For Example: given the values of σ and $\mathcal{E}$, then we can set σ to be the x-axis and $\mathcal{E}$ to be the y-axis (or vice versa). By plotting the corresponding values of each x and y, we are able to obtain the relationship between σ and $\mathcal{E}$. In other word, we can interpret Young's Modulus as $E = \frac{x}{y}$, where x and y represent the axis in a polar coordinate.

In general, Poisson's Ratio is the ratio of transverse strain to corresponding axial strain on a material stressed along one axis. In another word, given a sample object, then Poisson's Ratio is the ratio of the change in a sample width per unit width to the change in the length per unit length, as a result of straining the given sample. Below is the definition of Poisson's Ratio[6].

Definition 4.3. Define the *Poisson's Ratio* to be $\mathcal{V}$, then $\mathcal{V} = -\frac{\mathcal{E}_y}{\mathcal{E}_x}$, where $\mathcal{E}_y$ and $\mathcal{E}_x$ are the vertical (y) and horizontal (x) strains, respectively.

According to the equation of motion,

$$\rho h\frac{\partial^2 u_z}{\partial t^2} = \frac{h}{R}\frac{\partial}{\partial R}\left(\sigma_{RR}R\frac{\partial u_z}{\partial R}\right) + \frac{h\sigma_{\phi\phi}}{R^2}\frac{\partial^2 u_z}{\partial \phi^2} - \frac{Eh^3}{12(1-\mathcal{V}^2)}\nabla^4 u_z + q$$

where $q = q(R,\theta,t)$ is the contribution of external forces and displacements represented in cylindrical polar coordinate, E is Young's modulus (4.1), $\rho = \frac{M}{V}$ is the mass density (M is the mass of the modeled disc, whereas V is the volume of the disc), $\mathcal{V}$ is the Poisson ratio (4.3), and $\nabla^4 = (\nabla^2)^2$ where

$$\nabla^2 = \frac{\partial^2}{\partial R^2} + \frac{1}{R}\frac{\partial}{\partial R} + \frac{1}{R^2}\frac{\partial^2}{\partial \phi^2}$$

σ_{RR} is the PDE with respect to the length between a point and origin (R) and $\sigma_{\phi\phi}$ is the PDE with respect to the angle between x and R in the polar coordinate.

Before we define the next term, please recall that the *lagrangian coordinate* is any label that can uniquely identify a particle, which is mathematically denoted as a point in $\mathbb{R}^n$. *Eulerian coordinate*, on the other hand, fixates on a particular point in space, and records the properties of the fluid elements passing through that point. Mathematically, specify $\vec{V}(\vec{x}, t)$, where $\vec{V}$ is the velocity vector at time t. Therefore, given the lagrangian coordinate (4), we can obtain eulerian coordinate by $\vec{v}(\vec{x} = \vec{X}(\vec{X}_0, t), t) = \frac{d\vec{X}}{dt}(\vec{X}_0, t)$.

Since the essence of linear vibration analysis focuses on deriving and calculating the multidimensional function of which the time t takes to complete one circular motion, we will try to express the above results in terms of matrices composed of functions of t.

Definition 4.4. Mathematically, we specify the vector field $\vec{X}(\vec{X}_0, t)$, where $\vec{X}$ is the position vector of a particle at some time t and $\vec{X}_0$ is the position vector of the particle at some reference time, say $t = t_0$, and that is $\vec{X}_0 = \vec{X}(\vec{X}_0, t = t_0)$. Therefore, we define the *Lagrangian velocity* as the time derivative of the position vector following a particle $\vec{V} = \frac{d\vec{X}}{dt}$.

Based on the above equations and results, we are able to write the equations of motion of the plate in terms of the lagrangian coordinates (4) R and θ, and because the displacements of the rotation are assumed negligible, it is common to use a set of eulerian coordinates (4) r and θ to describe the equations of motion of the disc. Also, lagrangian coordinates and eulerian coordinate are related such that $r \approx R$, where they both are the length between a point and the origin, $\theta = \varphi + \Omega t$, and φ is the average circular motion of the disc. Then by rewriting the function of R, φ and using r, θ and t, we have: $f(R, \varphi, t) = f(r, \theta - \Omega t, t) = f'(r, \theta, t)$. Now, return to equation of motion and set $q = 0$, where q is the external forces exerted on the disc surface, we have

$$\rho h \frac{\partial u_z}{\partial t^2} + \frac{Eh^3}{12(1 - \mathcal{V}^2)} \nabla^4 u_z = 0$$

By comparing above equation to the original form of equation of motion, we have been able to cancel out most of the terms, such as $\frac{h}{R}\frac{\partial}{\partial R}\left(\sigma_{RR} R \frac{\partial u_z}{\partial R}\right)$ and $\frac{h\sigma_{\phi\phi}}{R^2}\frac{\partial^2 u_z}{\partial \phi^2}$, by using PDEs and coordinate transformation, and therefore, the matrix representations that we will obtain in the following section will be much simpler.

Next, we will continue to define a key term that will be crucial in terms of matrix multiplication, but before, recall that a matrix interpreted as a *Block Matrix* can be visualized as the original matrix with a collection of horizontal and vertical lines, which break it up, or partition it, into a collection of smaller matrices.

Moreover, the *Kronecker Product* (denoted by $\otimes$)[8] is an operation on two matrices of arbitrary size resulting in a block matrix, and notice that the Kronecker product is to be distinguished from the usual matrix multiplication, which is an entirely different operation.

Definition 4.5. If $\mathbf{A}$ is an $m \times n$ matrix and $\mathbf{B}$ is a $p \times q$ matrix, then the Kronecker product (4.5) $\mathbf{A} \otimes \mathbf{B}$ is the $pm \times qn$ block matrix (4) such that

$$\mathbf{A} \otimes \mathbf{B} = \begin{bmatrix} a_{11}\mathbf{B} & \cdots & a_{1n}\mathbf{B} \\ \vdots & \ddots & \vdots \\ a_{m1}\mathbf{B} & \cdots & a_{mn}\mathbf{B} \end{bmatrix}$$

Since we have begun to work with matrices right now, it is important to remember that in linear algebra, if T is a linear transformation from a vector space V over a field F into itself and $\mathbf{v}$ is a nonzero vector in V, then $\mathbf{v}$ is an eigenvector of T if $T(\mathbf{v})$ is a scalar multiple of $\mathbf{v}$. This can be written as

$$T(\mathbf{v}) = \lambda \mathbf{v}$$

where λ is a scalar in F, which is know as eigenvalue of $\mathbf{v}$. If the transformation is on the square matrix A and V is finite dimensional, then the above equation is equivalent to

$$A\mathbf{u} = \lambda \mathbf{u}$$

where where A is the matrix representation of T and $\mathbf{u}$ is the coordinate vector of $\mathbf{v}$[10]. The following definition will utilize the concepts of eigenvector and eigenvalue.

Definition 4.6. A pair of vectors, say $(\vec{u}, \vec{v}) \in \mathbb{R}^n \times \mathbb{R}^n$, is called *Eigenmodes* of the regular matrix $\mathbf{A}$ if for all $k \geq 0$

$$\mathbf{A} \otimes (k \times \vec{u} + \vec{v}) = (k+1) \times \vec{u} + \vec{v}$$

Then, notice that the frequencies to which they naturally respond are called *natural frequencies*[1]. In other word, it is the frequency generated without the interference of any other object. Mathematically, we can interpret such vibration using PDE. So the Newton's equation of motion becomes

$$ku = m\frac{d^2u}{dt^2}$$

where u represents the displacement of the mass from its equilibrium position and k is the stiffness of the object (mostly are modeled by springs). Therefore, this differential equation has two possible solutions such that $u = \sin(\omega t)$ or $u = \cos(\omega t)$ where $\omega = \sqrt{\frac{k}{m}}$ and $\frac{\omega}{2\pi}$ is the frequency in Hz.

Moreover, *nodal diameter*[11] is part of a frequency, and it can be considered as the number of waves, or also as the number of diameters in the structure along which the displacements are zero. *Note*: In order to calculate nodal diameter that occurs within a specific frequency, all we need to do is take the partial derivative of the equation of motion with respect to the time t.

Therefore, we can interpret its solution by sum of eigenmodes (4.6), and we have

$$\begin{aligned} u_z(R,\phi,t) = \sum_{n=0}^{\infty}\sum_{m=0}^{\infty} F_{mn}(R)\sin(\omega_{mn}t)(A_{mn}\sin(n\phi+\psi_n)) = \\ \sum_{n=0}^{\infty}\sum_{m=0}^{\infty} F_{mn}(R)\sin(\omega_{mn}t)(B_{mn}\sin(n\phi)+C_{mn}\cos(n\phi)) \end{aligned} \tag{1}$$

where $A_{mn}, B_{mn} = A_{mn}\sin(\psi_n), C_{mn} = A_{mn}\cos(\psi_n)$, and ψ_n are constants, and ω_{mn} is the natural frequency (4) of the system which has n nodal diameters (4) and m nodal circles parameters (obtained by πd, where d is the diameter)[7].

We can also write the Eulerian representations of Eq.1

$$\begin{aligned} \tilde{u}_z(r,\theta,t) = \sum_{n=0}^{\infty}\sum_{n=0}^{\infty} F_{mn}(r)\sin(\omega_{mn}t)(A_{mn}\sin(n\theta - n\Omega t+\psi_n)) = \\ \sum_{n=0}^{\infty}\sum_{n=0}^{\infty} F_{mn}\sin(\omega_{mn}t)(B_{mn}\sin(n\theta - n\Omega t)+C_{mn}\cos(n\theta - n\Omega t)) \end{aligned} \tag{2}$$

Note that both Eq.1 and Eq.2 express the vibration of the rotor during a typical braking operation, and based on Eq.1 and Eq.2, we obtain that the amplitude of vibration depends on the angle (ϕ or θ), radius of the disc (R or r), and braking time per operation (t). We will continue the discussion of these two equations and explore their solutions in the next section. Then, we will try to establish a relationship, if any, among these three variables based on linear vibration analysis.

5 Linear Vibration Analysis

The goal of linear vibration analysis in 3-D dimension is to determine the natural shapes and frequencies of an object or structure during free vibration. It is common to use the finite element method (FEM) to perform this analysis because, like other calculations using the FEM, the object being analyzed can have arbitrary shape and the results of the calculations are acceptable.

Remark 5.1. For this section, we will mainly focus on analyzing and deriving the solution for Eq.2 since the symbols contained in that equation make more sense mathematically (i.e r, θ, t).

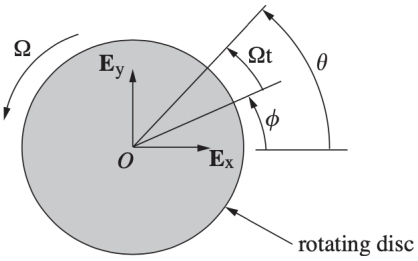

Figure 4: Schematic of a rotating disc and the angular co-ordinates θ and φ. The disc is assumed to be rotating counterclockwise at a constant speed Ω. The vectors $\mathbf{E}_x$, $\mathbf{E}_y$ and $\mathbf{E}_z = \mathbf{E}_x \times \mathbf{E}_y$ form an orthonormal, right-handed basis.

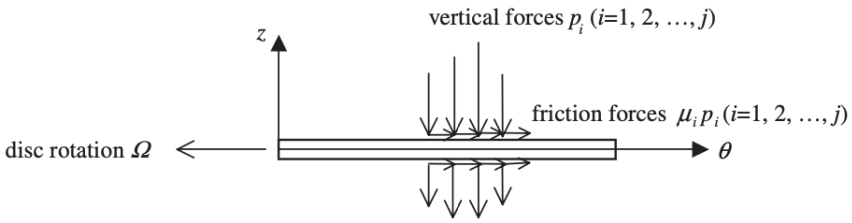

Figure 5: The forces acting onto the disc from the pads. Ω will be used as circular motion in this paper

Recall that in section 4, we have obtained the equation by using PDEs and coordinate transformation

$$\rho h \frac{\partial u_z}{\partial t^2} + \frac{Eh^3}{12(1-\mathcal{V})} \nabla^4 u_z = 0$$

where $\nabla^4 = (\nabla^2)^2$ and $\nabla^2 = \frac{\partial^2}{\partial R^2} + \frac{1}{R}\frac{\partial}{\partial R} + \frac{1}{R^2}\frac{\partial^2}{\partial \phi^2}$. Then, we will rewrite the expression of ∇^2 and replace R, ϕ with r, θ, and therefore, we have

$$\frac{\partial^2}{\partial r^2} + \frac{1}{r}\frac{\partial}{\partial r} + \frac{1}{r^2}\frac{\partial^2}{\partial \theta^2}$$

and since we know that $\nabla^4 = (\nabla^2)^2$, then ∇^4 can be also rewritten as

$$\left(\frac{\partial^2}{\partial r^2} + \frac{1}{r}\frac{\partial}{\partial r} + \frac{1}{r^2}\frac{\partial^2}{\partial \theta^2}\right)^2$$

Then, by using the similar strategy, we get the general solution for Eq.2 as

$$\tilde{u}(r, \theta, t) = \sum_{m=0}^{\infty} \sum_{n=-\infty}^{\infty} \psi_{mn}(r, \theta) q_{mn}(t)$$

This equation is crucial in terms of the brake squeal analysis. First of all, $\psi_{mn}(r, \theta)$ measures the vibration frequency based on different values of radius (denoted by r) and the angle of velocity (denoted by θ), $q_{mn}(t)$ is the centrifugal effect of modeled disc with respect to time t. Also, as it is defined in section 4, ψ_{mn} can be expressed in a equation composed of variables r and θ, so

$$\psi_{mn}(r, \theta) = \frac{R_{mn}(r)}{\sqrt{\rho h b^2}} \exp[(-1)^n (i\Omega t)] \tag{3}$$

where $R_{mn}(r)$ measures the initial circular motion of the disc with respect to the radius r, $\sqrt{\rho h b^2}$ calculates the overall volume of the brake system, and by moving $\frac{Eh^3}{12(1-\mathcal{V})}$ to the right hand side, we have

$$\rho h \frac{\partial u_z}{\partial t^2} + \frac{Eh^3}{12(1-\mathcal{V})} \nabla^4 u_z = 0 \Rightarrow \rho h \frac{\partial u_z}{\partial t^2} = -\frac{Eh^3}{12(1-\mathcal{V})} \nabla^4 u_z$$

Now, we take the double integral of Eq.3 and use $\tilde{\psi}_{kl}$ to represent the right hand side of Eq.3, which is $\frac{R_{mn}(r)}{\sqrt{\rho h b^2}}\exp(n\theta i)$, and we have

$$\int_0^{2\pi}\int_a^b \rho h\tilde{\psi}_{kl}\psi_{mn} r dr d\theta = \delta_{km}\delta_{ln}$$

where we set the boundary condition for $d\theta$ to be $[0, 2\pi]$, which is the entire surface of the disc within the cylindrical coordinate. Also, the boundary condition for dr is $[a, b]$ where it is the length from the origin to a given point on a disc. ρ is the weight of the disc and h is the thickness. δ_{km} is a differential equation resulted from the multiplication between $\tilde{\psi}_{kl}\psi_{mn}$, δ_{ln} is another differential function (different from δ_{km}).

Also note that generally, *Node*[11] represents the point that stays in the same position during the circular motion of a circle. In other words, the displacement of the point doesn't change, and *Nodal Circle*[1] counts the number of nodes (5) during a circular motion. Therefore, the number of nodes also indicates the overall circular velocity of the disc.

By substituting Eq.1, Eq.2, Eq.3 we have

$$\psi_{mn}(r,\theta) = \frac{R_{mn}(r)}{\sqrt{\rho h b^2}}\exp[(-1)^n(i\Omega t)] = -\frac{1}{\sqrt{\rho h b^2}}\sum_i^j R_{mn}(r_i)\exp[-il(\theta_i+\Omega t)]\left(1-\frac{\mu_i h}{2r_i}il\right)p_i \tag{4}$$

$$\psi_{mn}(r,\theta) = -\frac{1}{\sqrt{\rho h b^2}}\sum_i^j R_{mn}(r_i)\exp[-il(\theta_i+\Omega t)]\left(1-\frac{\mu_i h}{2r_i}il\right)p_i \tag{5}$$

where $l = 0, \pm1, \pm2, \cdots$ and other variables and equations are defined in previous paragraph. Since all of the functions and equations are multidimensional, and our goal is to generate the solution for each differential equation, so the best way to visualize and identify the solutions is to express all of the functions inside of a matrix.

Remark 5.2. For a given $\mathbf{D}$ where kl means the kth row and jth column such that

$$\mathbf{D} = \text{diag}[\frac{d^2}{dt^2} + 2\xi\omega_{kl}\frac{d}{dt} + \omega_{kl}^2]$$

then we could write $\mathbf{D}$ in the matrix form

$$\begin{bmatrix} \frac{d^2}{dt^2}+2\xi\omega_{11}\frac{d}{dt}+\omega_{11}^2 & 0 & 0 & \cdots & 0 \\ 0 & \frac{d^2}{dt^2}+2\xi\omega_{22}\frac{d}{dt}+\omega_{22}^2 & 0 & \cdots & 0 \\ 0 & 0 & \frac{d^2}{dt^2}+2\xi\omega_{33}\frac{d}{dt}+\omega_{33}^2 & \cdots & 0 \\ \vdots & \vdots & \vdots & \ddots & 0 \\ 0 & 0 & 0 & \cdots & \frac{d^2}{dt^2}+2\xi\omega_{kl}\frac{d}{dt}+\omega_{kl}^2 \end{bmatrix}$$

Here, since we are modeling the disc when its still, which means that R and t is 0, and so for the equation

$$\psi_{mn}(r,\theta) = \frac{R_{mn}(r)}{\sqrt{\rho h b^2}}\exp[(-1)^n(i\Omega t)]$$

we will have the constant 1, which will be the first number on the main diagonal. Then, notice that the linear vibration analysis only focuses on one specific point, which means that R will always be 0 since there is no displacement. Therefore, we are left with

$$\exp[(-1)^n(il\Omega t)]$$

then we define the upward vibration to be the even numbers and downward vibration to be the odd numbers, then we will neither obtain $\exp(-i\Omega t)$ or $\exp(i\Omega t)$, and the number of these two exponential functions depends on the total time t of the analysis. Therefore, we obtain the matrix

$$\text{diag}[\exp(-il\Omega t)] = \begin{bmatrix} 1 & 0 & 0 & 0 & 0 & 0 \\ 0 & \exp(-i\Omega t) & 0 & 0 & 0 & 0 \\ 0 & 0 & \exp(i\Omega t) & 0 & 0 & 0 \\ 0 & 0 & 0 & \exp(-i2\Omega t) & 0 & 0 \\ 0 & 0 & 0 & 0 & \exp(i2\Omega t) & 0 \\ \vdots & \vdots & \vdots & \vdots & 0 & \ddots \end{bmatrix} = (\text{diag}[\exp(il\Omega t)])^{-1}$$

Since matrix $\mathbf{D}$ is a diagonal matrix, then its eigenvalues are the elements on the diagonal, which are

$$1, \exp(-i\Omega t), \exp(i\Omega t), \exp(-i2\Omega t), \exp(i2\Omega t), \cdots$$

and note that all of the eigenvalues are exponential functions with variable t (i represents the ith row of the matrix and Ω is the circular velocity of the modeled disc), which means that if we want to minimize the vibration of the disc, which in return will optimize the brake squeal, we need to maximize the all of the exponential functions within a specific interval, and the interval is determined by the radius of the disc. Therefore, if we are given by a range of t, say in the interval $[a, b]$, we need to find

$$\max|\exp(-i\Omega t)|, \max|\exp(i\Omega t)|, \max|\exp(-i2\Omega t)|, \max|\exp(i2\Omega t)|, \cdots$$

where $t \in [a, b]$. Since we know that the maximum value for an exponential function given interval $t \in [a, b]$ is always going to be $t = b$ (the larger of the two), this is why we need to identify the t so that it is possible for a given point to complete a circular motion with specific Ω, which is the circular velocity. Because of the fact that we are modeling a single disc in this paper, then the best way to obtain the most accurate value for t is to calculate the average value for all t.

Also recall that in section 4, we define t to be the time that one disc takes to complete a circular motion, and based on the previous results we know that the larger the t gets, the smaller the vibration of the disc will be. If we fix a point on a disc, then this means that the time that the point takes to move around the disc should be increased.

Therefore, according to linear vibration analysis, we know that one of the most effective approaches for optimizing brake squeal is increase the overall size of the brake disc.

6 Conclusion and Future Research

Urban traffic congestion is a pressing issue worldwide, with its impact extending beyond travel delays to include environmental degradation, economic losses, and reduced quality of life. Addressing these challenges requires innovative and context-sensitive research to develop effective traffic management and efficiency strategies tailored to the unique conditions of highly congested cities in different countries. This section outlines a comprehensive plan for future research aimed at enhancing traffic efficiency in urban areas through data-driven solutions, emerging technologies, and multidisciplinary approaches.

6.1 Comparative Analysis of Urban Traffic Dynamics

Future research will focus on conducting comparative studies of traffic dynamics in highly congested cities across different countries. This will involve analyzing traffic flow patterns, intersection performance, and congestion hotspots in cities with varying population densities, infrastructure layouts, and traffic behaviors. By identifying regional and cultural differences, researchers can develop localized solutions that address specific challenges, such as unique vehicle compositions or driver behavior patterns.

6.2 Integration of Advanced Traffic Management Systems (ATMS)

A major focus will be the integration of advanced traffic management systems, including adaptive signal control, real-time traffic monitoring, and predictive analytics. Future studies will explore the deployment of intelligent transportation systems (ITS) that leverage machine learning algorithms and big data analytics to optimize traffic flow in real-time. Research will also examine the role of vehicle-to-infrastructure (V2I) communication in enhancing intersection efficiency and reducing delays.

6.3 Impact of Emerging Mobility Technologies

The adoption of emerging technologies, such as autonomous vehicles (AVs), connected vehicles (CVs), and electric vehicles (EVs), offers opportunities and challenges for urban traffic management. Future research will investigate the integration of these technologies into existing traffic systems, focusing on their impact on

intersection efficiency, congestion mitigation, and traffic safety. Scenarios involving mixed fleets of human-driven and autonomous vehicles will be modeled to understand transitional phases and identify optimal strategies for coexistence.

6.4 Sustainable Traffic Solutions for Developing Countries

In many developing countries, urban traffic congestion is exacerbated by limited infrastructure and rapidly increasing vehicle ownership. Future studies will prioritize cost-effective and sustainable solutions, such as public transportation optimization, non-motorized transport integration, and demand-responsive traffic management systems. These solutions will be tailored to resource-constrained environments while considering social and economic factors unique to these regions.

6.5 Environmental and Health Implications of Urban Traffic

Urban congestion contributes significantly to air pollution and greenhouse gas emissions. Future research will evaluate the environmental and public health impacts of traffic congestion, quantifying emissions at intersections and assessing the effectiveness of strategies such as congestion pricing, green wave signal timing, and increased adoption of EVs. The interplay between traffic efficiency and urban air quality will be a key focus area.

6.6 Human Behavior and Traffic Psychology

Human factors play a critical role in urban traffic efficiency. Future research will delve deeper into the psychological and behavioral aspects of drivers, cyclists, and pedestrians in highly congested urban environments. Studies will explore the impact of stress, decision-making under pressure, and cultural attitudes towards traffic laws on overall system performance. Insights gained will inform the design of driver education programs, signage, and enforcement strategies.

6.7 Leveraging Urban Data for Traffic Simulation and Prediction

The proliferation of smart city initiatives provides access to vast amounts of urban data. Future research will utilize this data to develop sophisticated traffic simulation models that replicate real-world conditions in highly congested cities. Predictive models incorporating historical data, weather conditions, and social events will help anticipate congestion patterns and enable proactive traffic management.

6.8 Policy and Governance for Traffic Efficiency

Effective traffic management requires strong policy frameworks and governance structures. Future studies will explore the role of policies, such as congestion pricing, carpooling incentives, and urban zoning regulations, in reducing congestion. Comparative analysis of successful policy interventions in different countries will provide a roadmap for governments and city planners seeking to implement evidence-based traffic solutions.

6.9 Cross-Disciplinary Collaborations

Traffic congestion is a complex issue that intersects with fields such as urban planning, engineering, environmental science, and public policy. Future research will emphasize cross-disciplinary collaborations to develop holistic approaches to traffic management. Partnerships with international organizations, local governments, and private sector stakeholders will be crucial in scaling solutions globally.

By addressing these research areas, future studies aim to develop innovative, equitable, and sustainable traffic management strategies tailored to the unique challenges of highly congested urban areas worldwide. The insights gained will inform global best practices, enhancing traffic efficiency and quality of life for urban residents.

References

[1] Q Cao et al. "Linear eigenvalue analysis of the disc-brake squeal problem". In: *International Journal for Numerical Methods in Engineering* 61.9 (2004), pp. 1546–1563.

[2] DA Crolla and AM Lang. "Paper VII (i) brake noise and vibration-the state of the art". In: *Tribology Series* 18 (1991), pp. 165–174.

[3] Duncan Dowson. "Bio-tribology". In: *Faraday Discuss.* 156 (0 2012), pp. 9–30. DOI: 10.1039/C2FD20103H. URL: http://dx.doi.org/10.1039/C2FD20103H.

[4] James D Halderman and Chase D Mitchell. *Automotive brake systems*. Prentice Hall, 1996.

[5] David V Hutton. *Fundamentals of finite element analysis*. McGraw-hill, 2004.

[6] N.M. Kinkaid, O.M. O'Reilly, and P. Papadopoulos. "Automotive disc brake squeal". In: *Journal of Sound and Vibration* 267.1 (2003), pp. 105–166. ISSN: 0022-460X. DOI: https://doi.org/10.1016/S0022-460X(02)01573-0. URL: https://www.sciencedirect.com/science/article/pii/S0022460X02015730.

[7] "DEDICATION". In: *Reference Data for Engineers (Ninth Edition)*. Ed. by Wendy M. Middleton and Mac E. Van Valkenburg. Ninth Edition. Woburn: Newnes, 2002, p. vii. ISBN: 978-0-7506-7291-7. DOI: https://doi.org/10.1016/B978-0-7506-7291-7.50056-X. URL: https://www.sciencedirect.com/science/article/pii/B978075067291750056X.

[8] "Front Matter". In: *Reference Data for Engineers (Ninth Edition)*. Ed. by Wendy M. Middleton and Mac E. Van Valkenburg. Ninth Edition. Woburn: Newnes, 2002, p. v. ISBN: 978-0-7506-7291-7. DOI: https://doi.org/10.1016/B978-0-7506-7291-7.50054-6. URL: https://www.sciencedirect.com/science/article/pii/B9780750672917500546.

[9] Masaaki Nishlwakl et al. *Study on disc brake squeal*. Tech. rep. SAE Technical Paper, 1989.

[10] Sebastian Oberst and JCS Lai. "Statistical analysis of brake squeal noise". In: *Journal of Sound and Vibration* 330.12 (2011), pp. 2978–2994.

[11] Huajiang Ouyang et al. "Numerical analysis of automotive disc brake squeal: a review". In: *International Journal of Vehicle Noise and Vibration* 1.3-4 (2005), pp. 207–231.

[12] Antti Papinniemi et al. "Brake squeal: a literature review". In: *Applied acoustics* 63.4 (2002), pp. 391–400.

[13] Antti Papinniemi et al. "Brake squeal: a literature review". In: *Applied Acoustics* 63.4 (2002), pp. 391–400. ISSN: 0003-682X. DOI: https://doi.org/10.1016/S0003-682X(01)00043-3. URL: https://www.sciencedirect.com/science/article/pii/S0003682X01000433.

[14] Willem Van den Heuvel and Alessandro Soncini. "NMR chemical shift as analytical derivative of the Helmholtz free energy". In: *The Journal of chemical physics* 138.5 (2013), p. 054113.